

# The effect of porosity on thermal conductivity of the porous NiTi SMA fabricated by SHS

MEHMET KAYA<sup>\*a</sup>, ABDULCELIL BUĞUTEKİN<sup>a</sup>, NURI ORHAN<sup>b</sup>

<sup>a</sup>Vocational School, Adiyaman University, 02040 Adiyaman, Turkey

<sup>b</sup>Metal Department, Technical Education Faculty, Firat University, 23119 Elazig, Turkey

In this study, porous NiTi shape memory alloy (SMA) was obtained by self-propagating high-temperature synthesis (SHS) of compacts prepared from elemental nickel and titanium powders and the effect of the porosity on the pore morphologies, microstructures and thermal conductivity of products synthesised after different cold compaction pressure was examined. The porosity in the synthesised products was in the range of 55.6–59.2 vol.%, with the green porosity being the primary source of final porosity. Green porosity (in other words cold compaction pressure) was found to have an effect on porosity, pore morphology of the synthesised products. Also, it was found that the thermal conductivity of the synthesised products increased with decreasing porosity.

(Received May 30, 2010; accepted August 12, 2010)

*Keywords:* Porous NiTi, Thermal conductivity, Fourier law, Shape memory alloy

## 1. Introduction

Shape Memory Alloys (SMAs) like NiTi are widely used as sensors and actuators regarding their ability to restore their original shape. NiTi also attracts a great deal of interest as a surgical implant material as well as a surgical instrument [1]. As the promising biomaterials for use as hard tissue implants, many porous NiTi-shape memory alloys (SMA) with different pore structures have been developed by combustion synthesis or self-propagating high-temperature synthesis (SHS) [2]. The cellular structure and mechanical properties of porous NiTi can resemble the characteristics of bone and as a result there has been interest in the application of the material in its porous state or as foam [1].

Self-propagating high-temperature synthesis (SHS), also known as combustion synthesis, is a method of synthesising many intermetallic compounds, particularly the aluminides of Ni and Ti, in a single process step within a short processing time (a few seconds to a few minutes) at high reaction temperatures (1500–4000 °C), viz. self-generation of energy. Homogeneous alloys of desirable stoichiometry can be synthesised by this route, thus eliminating the subsequent thermomechanical processing for homogenisation. This makes SHS an attractive alternative to the conventional powder metallurgy for material processing [3].

A few studies have been explored on the investigation of porous NiTi by SHS [2–6] so far. However, the thermal conductivity of porous NiTi has not been investigated yet. The thermal and electrical properties of shape memory alloys (SMA) are known to be different in their austenitic and martensitic phases [7]. Thermal conductivity is required to determine the feasibility and the basic design parameters of structural materials [8]. Therefore, in this study, porous NiTi SMA with different porosity was obtained by SHS of compacts prepared from elemental

nickel and titanium powders to investigate the effect of the porosity on thermal conductivity of porous products.

## 2. Experimental procedures

### 2.1. Specimen preparation

Commercial high purity powders of Ni and Ti (Ni; 99.8 wt-% and Ti; 99.5 wt-% purity, supplied by Alfa Aesar) with an average size of 44 μm were employed in this work. Firstly, the mixed powders of Ni and Ti with 50 at.-%Ni were blended in a rotating container for 24h for a homogenous mixture, and then the blended powder was pressed into cylindrical compacts of 10 mm in diameter using a hydraulic cold press at different compaction pressures of 50, 75 and 100 MPa. The green samples after compacting were preheated up to 200 °C with a heating rate of 15 °C/min in a furnace under the protection of high purity argon gas, and then they were subjected to electrical discharge pulse (14 kV and 30 mA) for a few seconds. The temperature of the green samples increased for a short time at the beginning of current application and ignition started.

Once ignited, combustion wave self-propagated along the axis of the specimen to the other end in a very short time, thus synthesising porous NiTi SMA [9].

### 2.2. Applied measuring techniques

#### 2.2.1. Microstructure examining

The porosity is determined by the formula,  $f = 1 - m/(dV)$ , where  $V$  and  $m$  refer to the volume and mass of the porous specimen respectively and  $d$  is theoretical density of it [9].

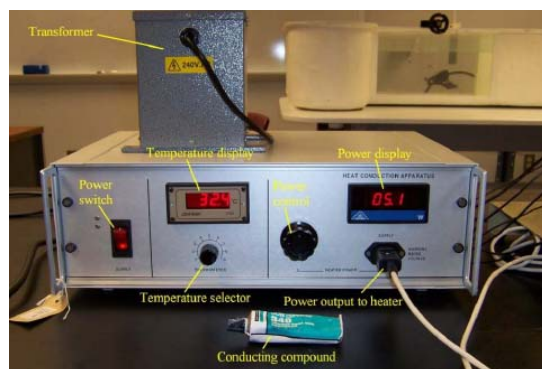
The general pore characteristics of the products were analysed using an optical microscope. The phase

constituents of fabricated specimen were determined by X-ray diffraction (XRD, Rigako Rad-B D-Max 2000 XRD) analysis using  $\text{CuK}\alpha$  radiation with  $1.54046 \text{ \AA}$ .

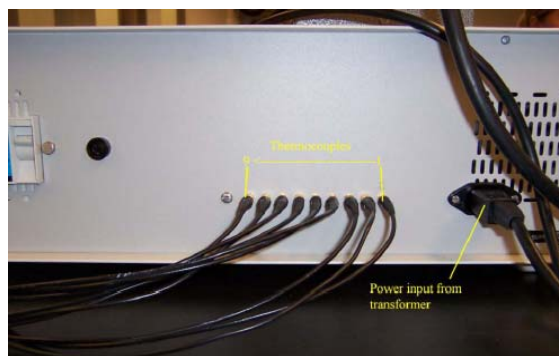
### 2.2.2. Thermal conductivity measurement

Thermal conductivity measurements of the specimens were tested with an H940 heat conduction unit (see setup, Fig. 1, a, b and c). The apparatus used in this experiment consists of three items. The first item is a transformer equipped with a circuit breaker. The transformer has two

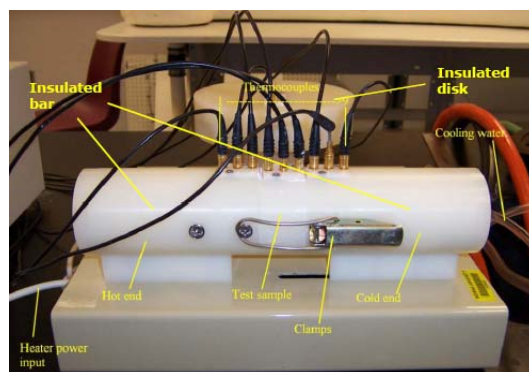
cords which connect it to an AC outlet and to the second item, the calibration unit. The calibration unit has two basic functions. It delivers power to the heater element within the test unit and it calibrates and displays the temperatures at nine locations along the test unit. The amount of power delivered to the test unit is controlled by the power control knob on the right side of the calibration unit; to its left is the temperature selector knob which is used to select one of the nine thermocouple temperatures for display on the digital readout, as shown in Figs. 1 (a) and (b) [10].



a)



b)



c)

Fig. 1. View of H940 heat conduction unit, (a) front view of calibration unit and transformer, (b) rear view of calibration unit, (c) front view of the test unit [10].

The third item is the test unit, which consists of two test geometries: an insulated brass bar which allows a sample to be placed between the two ends, and an insulated disk. Both geometries are equipped with a power supply, but we only used the insulated bar for this experiment. The test unit is also equipped with a cooling water hose. The purpose of the cooling water running through the unit at the cold end of the bar is to remove heat that is produced at the hot end and transferred by conduction to the cold end, keeping the cold end at a constant temperature. Once the rate at which heat is generated is equal to the rate at which heat is removed, steady state conditions (temperatures are fairly constant and readings can be taken) exist. The test unit has two heater cords: one from the test bar and the other from the test disk. Be sure to use only the heater cord for the bar, which connects to the heater plug located in the lower right hand corner of the calibration unit. Fig. 1(c) shows the front view of the test unit. In addition to this equipment, it is also found a box that contains the samples, thermocouples, and conducting paste in a small syringe. The samples can be placed in the bar test unit by releasing the clamps and sliding the cold end of the bar out. The thermocouples must be placed in order from 1 to 9 as shown in Figs. 1(b) and (c). The conducting paste is designed only to decrease contact resistance when applied to the ends of the connecting bars; it is not intended to enhance heat conduction [10].

Before the thermal conductivity measurements of the specimens were not tested, 316 stainless steel specimens whose thermal conductivity was known were tested to understand the accuracy of the measurements. The thermal conductivity of 316 stainless steel specimen was 14,8 W/mK at near room temperature and increased up to 18,2 W/mK with increasing temperature. These values are compatible with the literature [11]. The specimens were disk specimens of 10 mm in diameter and 5 mm in thickness. Firstly, the specimens were isolated with polyurethane spray about 1 mm in thick to prevent convection losses (also, protective boxes with heat-resistant were used to prevent heat losses), and then the both sides of specimens were polished to create good contact with the surfaces of brass plates. After, the specimens were placed between two brass plates, which one of them heated with power supply and the other cooled with running water. Thus, heat was transferred from brass heated to brass cooled. The experiments were occurred in air atmosphere. The temperature changes were measured with time by thermocouples. The thermocouples

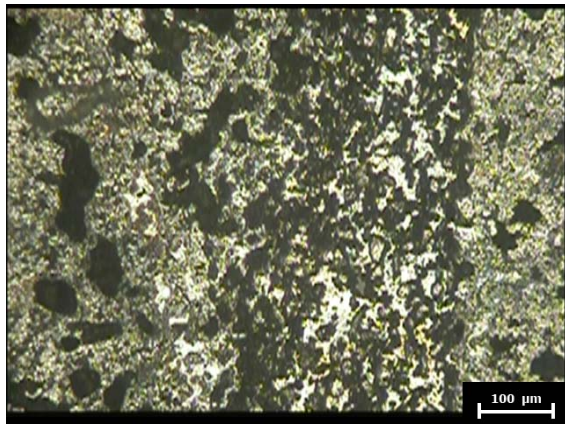
were placed at distances of 10 mm on the brass plates. Temperature values can read sensitivity ( $\pm 1$  °C) on digital screen, and power can control between 0-100 watt.

### 3. Results and discussion

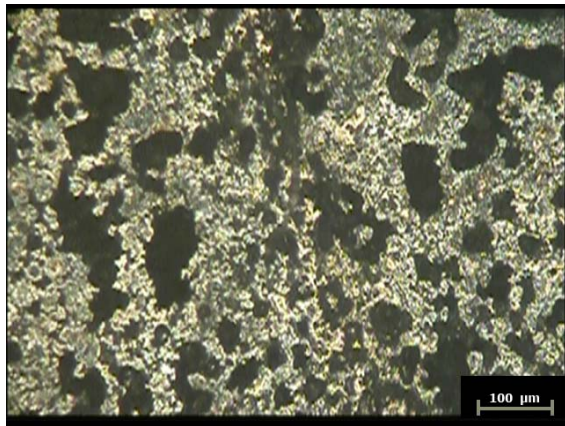
#### 3.1. Microstructure study

Fig. 2 a–c shows micrographs of porous specimens synthesised after different compaction pressures (50, 75, 100 MPa). There are many small closed and open pores in the NiTi matrix in Fig. 2. The pores are elliptic, circular or irregular in shape and porosity decreased with increasing cold compaction pressures. The porosity ratios are 59.2, 57.4 and 55.7 for the specimens cold compacted with pressures of 50, 75 and 100 MPa, respectively. Smaller pores were occurred when cold compaction pressure was 50 MPa, but pore sizes were increased with increasing cold compaction pressure. If it is desired to fabricate a porous NiTi SMA with low porosity and regular shape, higher preheating temperatures ( $\geq 200$  °C), higher cold compaction pressures (100 MPa) and lower heating rates ( $\leq 7$  °C) must be preferred. With heating rates higher than 20 °C/min, cold compaction pressures lower than 50 MPa and preheating temperatures higher than 450 °C, self-ignition occurred and the specimen deformed completely as a result of collapse in combustion channels in our experiments. Therefore, low preheating temperatures, low cold compaction pressures and a heating rate of 15 °C/min should be preferred in fabrication of high porous NiTi SMAs with a regular shape [12].

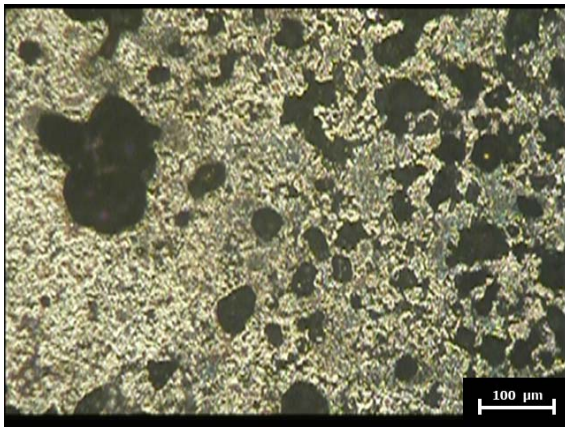
The XRD patterns of the porous NiTi SMAs with different cold compaction pressures are shown in Fig. 3. The desired products, such as B2(NiTi) and B19'(NiTi), are the predominant phases in the porous NiTi SMAs for all of the specimens. In addition, several second phases, such as  $Ti_2Ni$  and  $Ti_3Ni_4$ , also formed. Chu et al. [6] produced porous NiTi SMA with SHS method and determined the same phases seen from XRD results in this study. Tay et al. [3] showed that the intensity of B2(NiTi) increased and the intensities of the second phases decreased with increasing preheating temperature, but the effect of the green porosity on the intensity of the phases was not obvious. In this study, the effect of the green porosity (cold compaction pressure) on the intensity of the phases was not obvious, too.



a)



b)

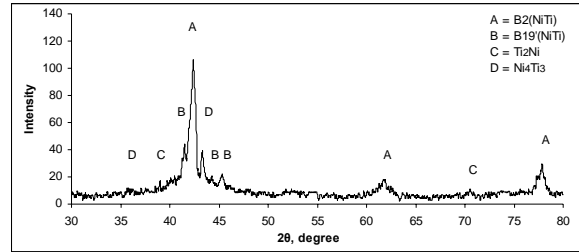


c)

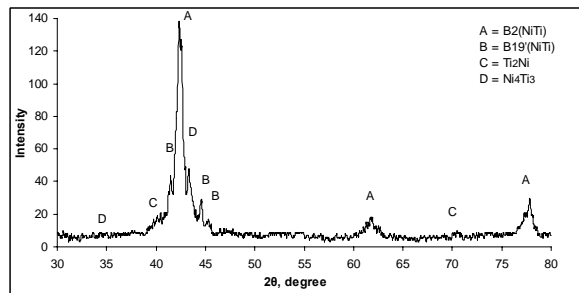
Fig. 2. Micrographs of porous NiTi synthesised at 200 °C after cold compacted, (a) 50 MPa, (b) 75 MPa, (c) 100 MPa.

Although the phases such as  $\text{Ni}_4\text{Ti}_3$  and  $\text{NiTi}_2$  usually form in porous NiTi alloys fabricated by SHS [6], the phases such as  $\text{Ni}_3\text{Ti}$ , pure Ni and pure Ti rarely occur [3].  $\text{Ni}_3\text{Ti}$ , pure Ni and pure Ti were not observed in this study. If the mixing is not homogeneous, the amount of undesired phases becomes larger. Since Ti powder is more flammable than Ni powder, could make the parent NiTi

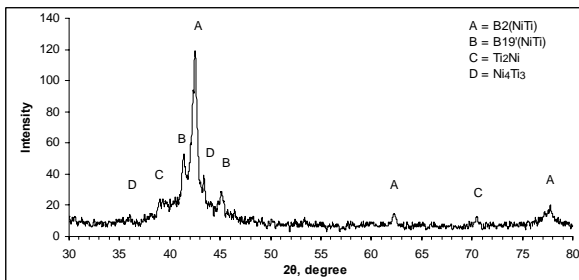
phase richer in Ni. Also, the presence of  $\text{Ti}_2\text{Ni}$  phase could make the parent NiTi phase richer in Ni, too. Thus the amount of undesired phases becomes larger [3,5,6].



a)



b)



c)

Fig. 3. XRD patterns of porous NiTi specimens synthesized after different cold compaction pressured, (a) 50 MPa, (b) 75 MPa (c) 100 MPa.

### 3.2. Thermal conductivity study

Thermal conductivities of specimens were determined with Fourier's law of heat conduction. Heat transfer refers to the energy transfer between two bodies due to temperature difference. The energy is transferred from the high temperature region to the low temperature region due to random molecular motion–diffusion. Higher temperatures are associated with higher molecular energies and when they collide with less energetic molecules the transfer of energy occurs [13].

The heat transfer rate by conduction can be expressed as:

$$\rho = -kA \frac{\partial T}{\partial X} \quad (1)$$

where,

$\rho$  – heat transfer rate (W)

$\frac{\partial T}{\partial X}$  - temperature gradient in the direction of the flow (K/m)

k – thermal conductivity of the material (W/mK)

A – cross-sectional area of heat path

Equation (1) is known as Fourier's law of heat conduction. Therefore, the heat transfer rate by conduction through the object in Fig. 1 can be expressed:

$$\rho = \frac{kA}{L} \Delta T_{12} \quad (2)$$

where,

A – cross-sectional area of the object

L – wall thickness

$\Delta T_{12}$  – temperature difference between two surfaces ( $\Delta T_{12} = T_1 - T_2$ )

k – thermal conductivity of object's material (W/mK)

To calculate the thermal conductivity of the specimens,  $\Delta T_{12}$  in Equation (2) is selected as  $\Delta T_{45} = T_4 - T_5$  (the closed points to sides of specimen). Fig. 4 shows the typical variations of temperatures with time within the specimens for  $T_4$  and  $T_5$  locations. The results indicate that the temperature variations between  $T_4$  and  $T_5$  locations increased directly with ascending time and after this the temperature variations were uniformed after about 120 min. In general, the steady-state temperatures were obtained after about 120 min. This time period is a function of the properties of specimen used, the heating rate, and the geometry of the apparatus. The thermal conductivities of the specimens were defined with Equation (2), using the temperatures and heating rates after this time period. The temperature variations between  $T_4$  and  $T_5$  locations increased with increasing porosity. These results indicate the thermal conductivities of the specimens decreased with increasing porosity. It was determined that the thermal conductivities were 4.8, 5.5 and 6.9 W/m<sup>2</sup>K for the specimen (a), (b) and (c), respectively. The thermal conductivity also changes with the phase constitutes of the specimens because the thermal conductivity of austenite phase is higher than that of the NiTi alloy existing multi phases [14,15]. The thermal conductivity of the solid NiTi wire existing B19'(NiTi) phase, martensite, is 14 W/(m<sup>2</sup>K) while the thermal conductivity of the solid NiTi wire existing B2(NiTi) phase, austenite, is 24 W/(m<sup>2</sup>K) [14]. In this study, it is seen that the thermal conductivities of the porous specimens are lower than that of solid specimen. This means that thermal conductivity was decreased by porosity. The similar results were determined by Zanotti et. al., which thermal conductivity was decreased with increasing porosity [15]. They determined that thermal conductivity for porous NiTi with %68, %48 and %30 were about 4, 3, 2 W/mK, respectively. These values are lower than the ones determined in this study, because their specimens contain multi phases. Also the experimental

conditions of the measurements are different with in this study.

Table 1. Typical variations of temperatures and thermal conductivity with time within the specimens with different porosity.

Sample	Heat rate (watt)	T <sub>4</sub> (°C)	T <sub>5</sub> (°C)	k(W/mK)
% 59.2 porosity	9.7	141.2	14.6	4.8
% 57.4 porosity	9.7	126.5	15.1	5.5
% 55.7 porosity	9.7	104.9	15.2	6.9

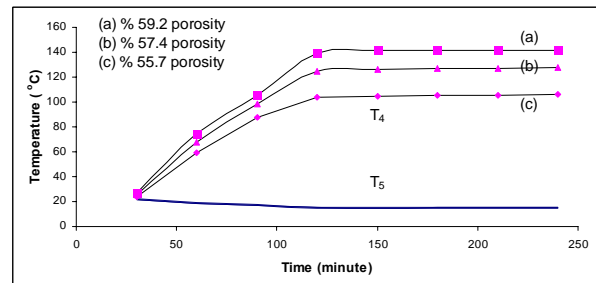


Fig. 4. Typical variations of temperatures with time within the specimens with different porosity for  $T_4$  and  $T_5$  locations; (a), (b) and (c) are typical variations curves of temperatures for the specimens with % 55.7, % 57.4 and % 59.2 porosity.

## 5. Conclusion

Porous NiTi SMAs free from pure Ni, pure Ti and Ni<sub>3</sub>Ti phases were fabricated by SHS. B2(NiTi) and B19'(NiTi) phases were predominant also the second phases such as Ni<sub>4</sub>Ti<sub>3</sub>, Ti<sub>2</sub>Ni were occurred in the microstructure of the specimens. The distribution of the pores was uniform and most of the pores were isolated and rarely interconnected. The porosity was decreased with increasing cold compaction pressure, but it was fully not observed the effect of cold compaction pressure on the phase constitutes. Thermal conductivity of the synthesised products increased with decreasing porosity. In addition, it was seen that the thermal conductivities of the porous specimens were lower than that of solid NiTi alloy.

## References

- [1] C. Zanotti, P. Giuliani, P. Bassani, Z. Zhang, A. Chrysanthou, *Intermetallics* **18**, 14–21 (2010).
- [2] C. L. Chu, C. Y. Chung, P. H. Lin, *Materials Letters* **59**, 404–407 (2005).
- [3] B. Y. Tay, C. W. Goh, Y. W. Gu, C. S. Lim, M. S. Yong, M. K. Ho, M. H. Myint, *Journal of materials processing technology*, **202**, 359–364 (2008).
- [4] M. Kaya, N. Orhan, B. Kurt, *Powder Metallurgy*,

- 52** (1), 36-41 (2009).
- [5] C. Shearwood, Y. Q. Fu, L. Yu, K. A. Khor, *Scr. Mater.* **52**, 455–460 (2005).
- [6] C. L. Chu, C. Y. Chung, P. H. Lin, S. D. Wang, *J. Mater. Process. Technol.* **169**, 103–107 (2005).
- [7] *Smart Mater. Struct.* **9**, 632–639 (2000). Printed in the UK, M. G. Faulkner, J. J. Amalraj and A. Bhattacharyya.
- [8] Y. Terada, K. Ohkubo, S. Miura, J. M. Sanchez, T. Mohri, *Journal of Alloys and Compounds*, **354**(1-2), 202–207 (2003).
- [9] M. Kaya, N. Orhan, G. Tosun, *Current Opinion in Solid State and Materials Science*, **14**(1), 21-25 (2010).
- [10] P. A. Hilton LTD., <<Kondüksiyonla ısı iletim cihazı Deney işlemleri bakım kitabı>>, Ağustos 1994.
- [11] L. J. Ott, R. A. Hedrick, ORTCAL- A Code for THTF Heater Rod, Thermocouple Calibration, Oak Ridge national laboratory, (1979), 217.
- [12] M. Kaya, N. Orhan, G. Tosun, *Materials Science and Technology*, DOI 10.1179/174328409X410809, 2009.
- [13] A. Buğutekin, B. Köse, A. K. Binark, M. O. Isikan, *Application Insulation Technologies Congress*, 875-879 (2005) İstanbul -Turkey.
- [14] M. G. Faulkner, J. J. Amalraj, A. Bhattacharyya, *Smart Material Structure* **9**, 632–639 (2000). Printed in the UK.
- [15] C. Zanotti, P. Giuliani, P. Bassani, Z. Zhang, A. Chrysanthou, *Intermetallics*, **18**(1), 14–21 (2010).

---

\*Corresponding author: mkaya@adiyaman.edu.tr